Journal of Computational Methods in Sciences and Engineering 14 (2014) 17–28
DOI 10.3233/JCM-130481
IOS Press

Theoretical analysis of external noise and bistability in the catalytic CO oxidation on Pd(111)

Miguel Pineda[a,*] and Raúl Toral[b]
[a]*Department of Physics, Universidad Simón Bolívar, Caracas, Venezuela*
[b]*Instituto de Física Interdisciplinar y Sistemas Complejos (CSIC-UIB), Palma de Mallorca, Spain*

Abstract. We theoretically study the impact of an external noise on a kinetic mean-field model for the bistable catalytic CO oxidation on Pd(111) surfaces. A spatially homogeneous Gaussian white noise is imposed on the fraction of CO in the constant gas flow directed at the surface and the resulting stochastic system is analyzed by a set of Langevin equations. Using an adiabatic elimination technique, we are able to analyze the interplay between the noise and the kinetic bistability reported for this surface reaction in recent experimental studies. The analytical results predict a strong impact on the bistability phase diagram. The stochastic effects are analyzed by computing stationary solutions of the probability distribution functions and the transition times between the active and inactive states of the bistable region. We also introduce an effective potential description that allows us to analyze the impact of noise.

Keywords: CO oxidation, bistability, noise, effective potential

1. Introduction

Unexpected phenomena can emerge when strong nonlinearities act together with stochastic fluctuations or noise [1]. A counterintuitive result that has generated much attraction last years is that noise might induce new ordering phenomena by allowing a dynamical system to explore regions of the phase space that are not accessible to the deterministic version of the dynamics. A convenient class of systems to study these interesting phenomena are chemical reactions on solid surfaces, among which the catalytic oxidation of carbon monoxide on platinum-group metal surfaces has found special attention, both from the experimental and theoretical points of view [2,3]. The most prominent application of this reaction is the three-way automotive catalysis, where the toxic CO is transformed in carbon dioxide by a car's catalytic converter. This reaction is also one of the simplest realizations of chemical reactions on single crystal surfaces and has been used in the last decades to analyze many dissipative structures. For example, it has been found that this surface reaction exhibits a great variety of nonlinear phenomena, such as self-sustained kinetic oscillations, bistability, chaos, and spatiotemporal patterns [2,3].

Despite many inherent difficulties, several experimental studies of noise-induced phenomena in the nonlinear behavior of the catalytic CO oxidation have been reported in recent years [4–8]. Along

*Corresponding author: Miguel Pineda, Department of Physics, Universidad Simón Bolívar, Caracas 1080, Venezuela. E-mail: mpineda@fis.usb.ve.

these lines, the experimentalists often consider separately the effects of molecular noise occurring on nanoscale surfaces (internal noise) and stochastic fluctuations imposed on the external control parameters (external noise). In particular, the experimental characterization of external noise-induced effects in surfaces reactions is very difficult and only few experimental studies have been reported. For example, the catalytic CO oxidation on Ir(111) was studied in a fashion where the total CO+O_2 flux was held constant. It was demonstrated that the interplay between a superposed external noise and the bistable behavior of this catalytic surface reaction induces transitions between the two stable steady states via island nucleation and growth. The experimental results were partially explained by numerical simulations of a set of reaction-diffusion equations under spatiotemporal noise [9]. The emergence of spatiotemporal structures in the CO oxidation on Pt(110) under a spatially homogeneous or global noise has been also experimentally studied [8]. The authors of that work interpreted the effects of noise as a control mechanism of the many different patterns observed on this surface, and in order to interpret the experimental results, they performed simulations by using a set of reaction diffusion equations under spatially homogeneous noise. However, while mainly numerical simulations of those systems have been performed, few analytical studies of external noise affecting the kinetic bistability of CO oxidation have been reported. The aim of this work is to present a theoretical analysis of a global external noise added to a kinetic mean-field model for the catalytic CO oxidation on the structurally stable Pd(111) surfaces.

Though it has been known for many years that the catalytic oxidation of carbon monoxide on Pd(111) surfaces follows the Langmuir-Hinshelwood (LH) mechanism [10], it was only recently that a true bistable behavior was experimentally reported for this surface [11]. The experimental studies were performed in a fashion where the total CO+O_2 flux ($\phi = \phi_{\rm CO} + \phi_{\rm O}$) was held constant and CO ($Y = \phi_{\rm CO}/\phi$) and O_2 ($1 - Y$) partial contributions varied. For temperatures below $T_c \approx 450K$, it was found that two stationary steady states coexist for a range $Y^- < Y < Y^+$. This bistable behavior is characterized by a reaction hysteresis where a branch with high CO_2 formation (active steady state) on a predominately oxygen covered surface and a branch of low CO_2 formation (inactive steady state) on a mainly CO covered surface, coexist. In several subsequent experiments [12], rare transitions between the two stationary steady states, induced by weak noise created by mass flow controllers, were observed. To shed light on these experimental results, this contribution analyzes the impact of a spatially homogeneous Gaussian white noise on this kinetic bistability.

The rest of the paper is organized as follows. The model with external global noise is presented in Section 2. Section 3 introduces the one component model obtained after adiabatic reduction of oxygen coverage. The impact of noise on the bistable region is analyzed in Section 4. Summary and conclusions are presented in Section 5.

2. The model with external global noise superposed on the CO fraction

On palladium, the catalytic CO oxidation proceeds via the LH mechanism which can be schematically expressed as follows [2]:

$$CO(\text{gas}) + * \underset{k_2}{\overset{k_1}{\rightleftarrows}} CO(\text{ads}),$$

$$O_2(\text{gas}) + 2* \xrightarrow{k_4} 2O(\text{ads}),$$

$$CO(\text{ads}) + O(\text{ads}) \overset{k_3}{\longrightarrow} CO_2(\text{gas}) + 2*,$$

with * and (ads) denoting a vacant adsorption site and adsorbed molecules or adatoms, respectively. The reactants first adsorb on the surface, diffuse to adjacent adsorption sites, and then react in the adsorbed state from where the product desorbs instantaneously. The reaction processes schematically represented above occur at the indicated rates k_1, k_2, k_3, and k_4.

Motivated by the experiments mentioned in the introduction, we consider a kinetic model where an external global noise is imposed on the CO fraction Y of the total CO+O_2 flux ϕ directed to the surface. Basically, noise is superposed on Y, i.e., $Y \longrightarrow Y + \eta(t)$, where $\eta(t)$ is Gaussian white noise with the following properties $\langle \eta(t) \rangle = 0$ and $\langle \eta(t)\eta(t') \rangle = r^2 \delta(t - t')$. Here, r represents the intensity of noise. Though we expect a rich variety of spatial structures generated in this reaction under noise, in this work we will focus on stochastic effects on the bistability phase diagram that can be explained without modeling macroscopic diffusion [11,12]. Under this approximation, oxygen and CO are very mobile and there are no gradients. Thus, after taking into account the reactions steps together with these assumptions, the mean-field Langevin equations for the surface concentration $\theta_{\rm CO}$ of CO(ads) and $\theta_{\rm O}$ of O(ads) in units of monolayers (ML) are

$$\frac{d\theta_{\rm CO}}{dt} = f^{\rm CO}(\theta_{\rm CO}, \theta_{\rm O}) + g^{\rm CO}(\theta_{\rm CO})\eta(t), \tag{1}$$

$$\frac{d\theta_{\rm O}}{dt} = f^{\rm O}(\theta_{\rm CO}, \theta_{\rm O}) + g^{\rm O}(\theta_{\rm CO}, \theta_{\rm O})\eta(t), \tag{2}$$

where

$$\begin{aligned} f^{\rm CO}(\theta_{\rm CO}, \theta_{\rm O}) &= k_1 Y(1 - \theta_{\rm CO}) - k_2 \theta_{\rm CO} - k_3 \theta_{\rm CO}\theta_{\rm O}, \\ g^{\rm CO}(\theta_{\rm CO}) &= k_1(1 - \theta_{\rm CO}), \end{aligned} \tag{3}$$

and

$$\begin{aligned} f^{\rm O}(\theta_{\rm CO}, \theta_{\rm O}) &= k_4(1 - Y)(1 - \theta_{\rm CO} - \theta_{\rm O})^2 - k_3 \theta_{\rm CO}\theta_{\rm O}, \\ g^{\rm O}(\theta_{\rm CO}, \theta_{\rm O}) &= -k_4(1 - \theta_{\rm CO} - \theta_{\rm O})^2, \end{aligned} \tag{4}$$

with $k_1 = S_{\rm CO}\phi$ and $k_4 = 2S_{\rm O}\phi$. The parameters $S_{\rm CO}$ and $S_{\rm O}$ are the initial sticking coefficients for CO and O_2 on Pd(111), respectively, and ϕ is the total CO+O_2 flux to the surface. The absorption terms presented in $f^{\rm CO}(\theta_{\rm CO}, \theta_{\rm O})$ and $f^{\rm O}(\theta_{\rm CO}, \theta_{\rm O})$ consider the empirical fact that while preadsorbed CO inhibits dissociative adsorption of oxygen, no such site-blocking effect is exerted by O(ads) on incoming CO molecules [11]. Finally, $k_2 = \nu_d e^{-E_d/RT}$ and $k_3 = \nu_r e^{-E_r/RT}$. For parameters we use the values $\phi = 1$ ML s^{-1}, $S_{\rm CO} = 0.8$, $\nu_d = 5 \times 10^{13}$ s^{-1}, $E_d = 125$ kJ/mol, $\nu_r = 10^7$ s^{-1}, $E_r = 53$ kJ/mol, and $S_{\rm O} = 0.5$ [11,12]. We shall use the Stratonovich interpretation to analyze the system of Langevin equations [13] and note that the same noise variable $\eta(t)$ appears in both equations. Though the impact of the spatially homogeneous noise can be analyzed by direct numerical integration of these stochastic equations [13,14], in this work we will show that solutions can be found by introducing appropriated approximations. In the case of no noise, or $r = 0$, Eqs (1)–(2) represent the deterministic differential equations proposed by Karpitschka et al. [11] to qualitative reproduce the bistable behavior observed in experiments.

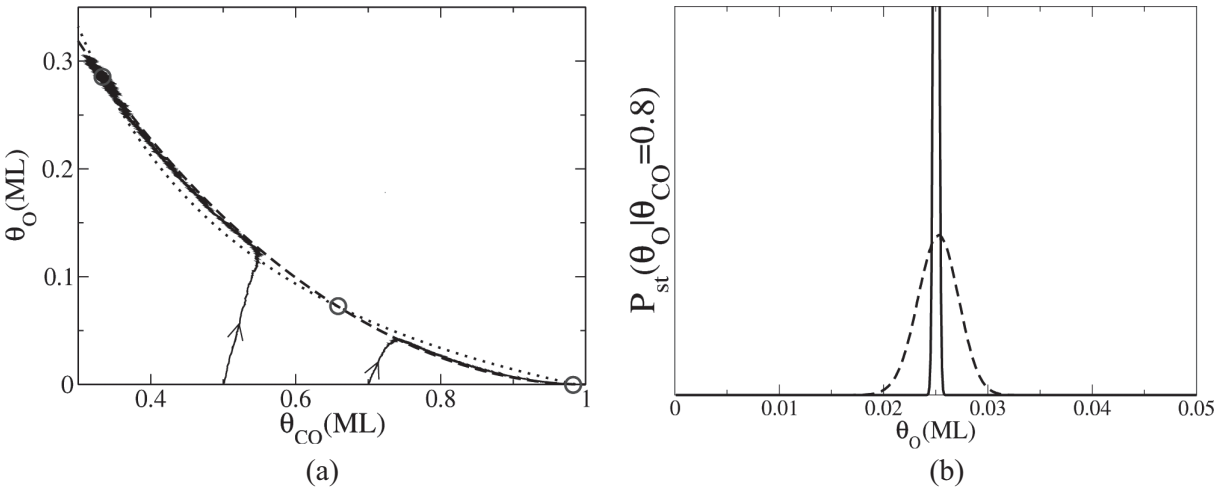

Fig. 1. (a) Phase-space of the deterministic nullclines $d\theta_{\rm O}/dt$ (dashed line) and $d\theta_{\rm CO}/dt$ (dotted line) obtained inside the bistable region for $r = 0.0$. Open circles represent the steady state solution of the system. The two extreme circles are the stable active and inactive states with low and high CO concentration, respectively. The intermediate circle is the unstable solution or separatrix point. For $r = 0.01$, two stochastic trajectories for different initial conditions are also presented (black solid lines). The oxygen nullcline with low oxygen concentration is rapidly reached from any initial condition. Hence $\theta_{\rm O}$ is the fast variable which can be adiabatically removed from the original system. (b) The stationary conditional probability distribution of oxygen for $\theta_{\rm CO} = 0.8$. This probability distribution is peaked and unimodal around $\langle\theta_{\rm O}\rangle = \overline{\theta}_{\rm O} = 0.025$ for $r = 0.01$ (solid line) and 0.1 (dashed line). The CO partial pressure and the temperature of the surface are fixed at $Y = 0.2141$ and $T = 400K$, respectively.

3. Adiabatic reduction: The one-component model

The adiabatic elimination of fast variables is a well established technique to reduce high dimensional deterministic systems [15]. It can be also extended to high dimensional stochastic systems [16,17]. To analyze the stochastic aspects of the bistable catalytic CO oxidation on Pd(111) surfaces, in this work we use a reduction method recently proposed in [18]. The starting point of this method is to identify in the model represented by Eqs (1) and (2) the fast and the slow variables. This can be done by direct numerical integration of those equations for small noise intensities, which reveals that a slowly varying trajectory in phase space with low and almost constant oxygen coverage is rapidly reached from any initial condition, which nearly coincides with the deterministic nullcline $d\theta_{\rm O}/dt = 0$ (see Fig. 1(a)). Hence $\theta_{\rm O}$ is the fast variable. Then, the main point is to perform the adiabatic elimination of this variable from the original set of stochastic differential equations. To do that, let us introduce the joint probability density function (pdf) to have $\theta_{\rm CO}$ and $\theta_{\rm O}$ at a given time as

$$P(\theta_{\rm CO}, \theta_{\rm O}; t) = P(\theta_{\rm CO}; t) P(\theta_{\rm O}|\theta_{\rm CO}; t), \tag{5}$$

where $P(\theta_{\rm O}|\theta_{\rm CO}; t)$ is the conditional probability density to get the value $\theta_{\rm O}$ for fixed $\theta_{\rm CO}$ at time t, and $P(\theta_{\rm CO}; t)$ is the probability density to get $\theta_{\rm CO}$ at the same time. For a fixed value $\theta_{\rm CO}$, we also assume that $P(\theta_{\rm O}|\theta_{\rm CO}; t)$ rapidly relax towards a monomodal sharply peaked function [see Fig. 1(b)]. In this approximation the maximum of the steady state probability distribution, $\overline{\theta}_{\rm O}$, coincides with the average value $\langle\theta_{\rm O}\rangle$.

For a fixed $\theta_{\rm CO}$, the equation for the average value of oxygen concentration is

$$\frac{d\langle\theta_{\rm O}\rangle}{dt} = \langle f^{\rm O}(\theta_{\rm CO}, \theta_{\rm O})\rangle + \langle g^{\rm O}(\theta_{\rm CO}, \theta_{\rm O})\eta(t)\rangle. \tag{6}$$

Then, using Novikov's theorem [19] for the noise term, we get the following effective deterministic equation for the oxygen concentration

$$\frac{d\overline{\theta}_{\rm O}}{dt} = f^{\rm O}(\theta_{\rm CO}, \overline{\theta}_{\rm O}) + \frac{r^2}{2} g^{\rm O}(\theta_{\rm CO}, \overline{\theta}_{\rm O}) \frac{\partial g^{\rm O}(\theta_{\rm CO}, \overline{\theta}_{\rm O})}{\partial \overline{\theta}_{\rm O}}, \tag{7}$$

where, as mentioned above, we adopt $\overline{\theta}_{\rm O} = \langle \theta_{\rm O} \rangle$.

As we have argued that $\theta_{\rm O}$ is the fast variable, we make the assumption that the value of the concentration $\overline{\theta}_{\rm O}$ as a function of $\theta_{\rm CO}$ can be obtained from setting $\frac{d\overline{\theta}_{\rm O}}{dt} = 0$ in the previous equation. This yields a relation $\overline{\theta}_{\rm O}(\theta_{\rm CO})$ than can be replaced in Eq. (1) and allows us the reduction of the problem to the following one-component Langevin equation for $\theta_{\rm CO}$

$$\frac{d\theta_{\rm CO}}{dt} = F^{\rm CO}(\theta_{\rm CO}) + g^{\rm CO}(\theta_{\rm CO})\eta(t), \tag{8}$$

where we use the notation $F^{\rm CO}(\theta_{\rm CO}) = f^{\rm CO}(\theta_{\rm CO}, \overline{\theta}_{\rm O}(\theta_{\rm CO}))$. Using standard techniques, it is possible now to write down the Fokker Planck equation for the pdf $P(\theta_{\rm CO}; t)$ as

$$\begin{aligned} \frac{\partial P(\theta_{\rm CO}; t)}{\partial t} = & -\frac{\partial \left[F^{\rm CO}(\theta_{\rm CO}) P(\theta_{\rm CO}; t)\right]}{\partial \theta_{\rm CO}} + \\ & \frac{r^2}{2} \frac{\partial}{\partial \theta_{\rm CO}} \left[g^{\rm CO}(\theta_{\rm CO}) \frac{\partial \left[g^{\rm CO}(\theta_{\rm CO}) P(\theta_{\rm CO}; t)\right]}{\partial \theta_{\rm CO}} \right], \end{aligned} \tag{9}$$

from where it follows that the steady state solution is given by

$$P_{\rm st}(\theta_{\rm CO}) = \frac{N}{g^{\rm CO}(\theta_{\rm CO})} \exp\left[\int_0^{\theta_{\rm CO}} \frac{2F^{\rm CO}(\theta)}{r^2 \left[g^{\rm CO}(\theta)\right]^2} d\theta \right], \tag{10}$$

where N is the normalization constant. This is usually interpreted in terms of an effective potential $V(\theta_{\rm CO})$ as $P_{\rm st}(\theta_{\rm CO}) = N \exp[-V(\theta_{\rm CO})]$ or,

$$V(\theta_{\rm CO}) = -\int_0^{\theta_{\rm CO}} \frac{2F^{\rm CO}(\theta)}{r^2 \left[g^{\rm CO}(\theta)\right]^2} d\theta + \ln g^{\rm CO}(\theta_{\rm CO}). \tag{11}$$

The corresponding steady state maxima $\overline{\theta}_{\rm CO}$ correspond to the minima of the effective potential, satisfying:

$$V'(\overline{\theta}_{\rm CO}) = 0. \tag{12}$$

In the following sections we will use these expressions to analyze some of the phenomena induced by the external global Gaussian white noise on the bistable behavior of the catalytic CO oxidation on Pd(111) surfaces.

4. Impact of external noise on the bistable bifurcation diagram

By determining whether Eq. (12) has one or more solutions, we can obtain the bistability phase diagram in the parameter space (T, Y) as function of the noise intensity r. Bistable regions appear at the set of parameters for which two stable (minima of the potential) solutions of Eq. (12) are separated by an

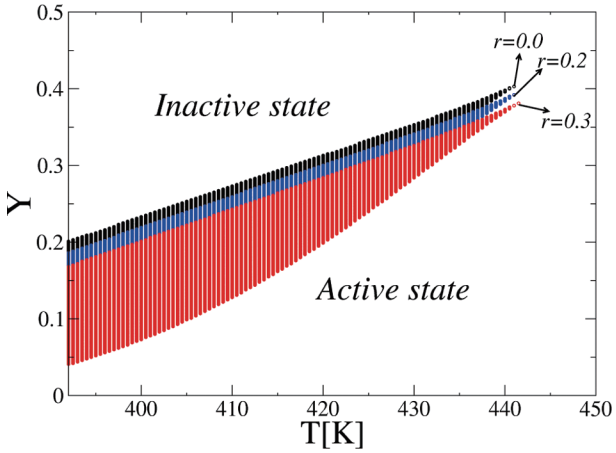

Fig. 2. Phase diagram for the bistable CO oxidation on Pd(111) for different noise intensities plotted in the plane spanned by the CO fraction Y and the surface temperature T. The dotted colored regions correspond to bistability as obtained from Eqs (7) and (12) with $\frac{d\overline{\theta}_{\rm O}}{dt} = 0$ for noise intensities $r = 0.0$ (black region), 0.2 (blue region), and 0.3 (red region). Outside the bistable region the reactive and inactive states exist. The comparison of the three regions shows that a shift of the global bifurcation diagram occurs when the noise intensity varies.

unstable one (maximum of the potential). As mentioned above, the deterministic version of the model ($r = 0$) is characterized by a bistable behavior for temperatures smaller than a characteristic value T_c. This nonequilibrium bistability is constrained by two saddle node bifurcations occurring at certain critical values of Y and disappears as $T \to T_c$ [11]. Figure 2 clearly shows that indeed a shift of this bistable region occurs as a function of the noise intensity r. It basically means that, under the influence of an external global noise, the positions of the saddle node bifurcation lines and the cusp bifurcation point change in the parameter space.

4.1. Probability distributions and transition times: A two-well effective potential

In this section, to analyze the impact of noise we use the probability distribution and effective potential derived in Section 3. We will assume that the probability distribution $P(\theta_{\rm CO}, t)$ approaches Eq. (10) which includes transitions between the two stable states of the bistable region. One interesting consequence of external noise is that when it acts on nonlinear systems, the number of maxima of the stationary probability distributions may change as a function of the noise intensity [1]. To verify that this shift is present in the bistability phase diagram predicted above, Fig. 3 shows $P_{\rm st}(\theta_{\rm CO})$ and $V'(\theta_{\rm CO})$ for two values of noise intensity r with a surface temperature set at $T = 435K$. We consider two values of partial pressure Y just around the saddle node bifurcation lines (the borders of the bistable region). The inset of Fig. 3(a) shows $V'(\theta_{\rm CO})$ for $Y = 0.370$ (upper saddle node bifurcation line) for noise intensities $r = 0.1$ (red solid line) and $r = 0.2$ (blue dotted line). In the first case the intersections with the black dashed line indicate that $V(\theta_{\rm CO})$ has two minima (corresponding to stable solutions) separated by a maximum or unstable solution, a situation of bistability. One stable solution corresponds to a high concentration of carbon monoxide ($\theta^h_{\rm CO}$) and the other one to a low concentration of CO ($\theta^l_{\rm CO}$). The unstable solution ($\theta^u_{\rm CO}$) is placed between the two stable solutions. This result clearly means that $P_{\rm st}(\theta_{\rm CO})$ has two maxima separated by a minimum, with transitions between the two maxima induced by external noise (main figure, black dashed line). However, when noise intensity increases to $r = 0.2$, we get that $V(\theta_{\rm CO})$ has only one minimum, and therefore, the probability distribution presents a monomodal shape

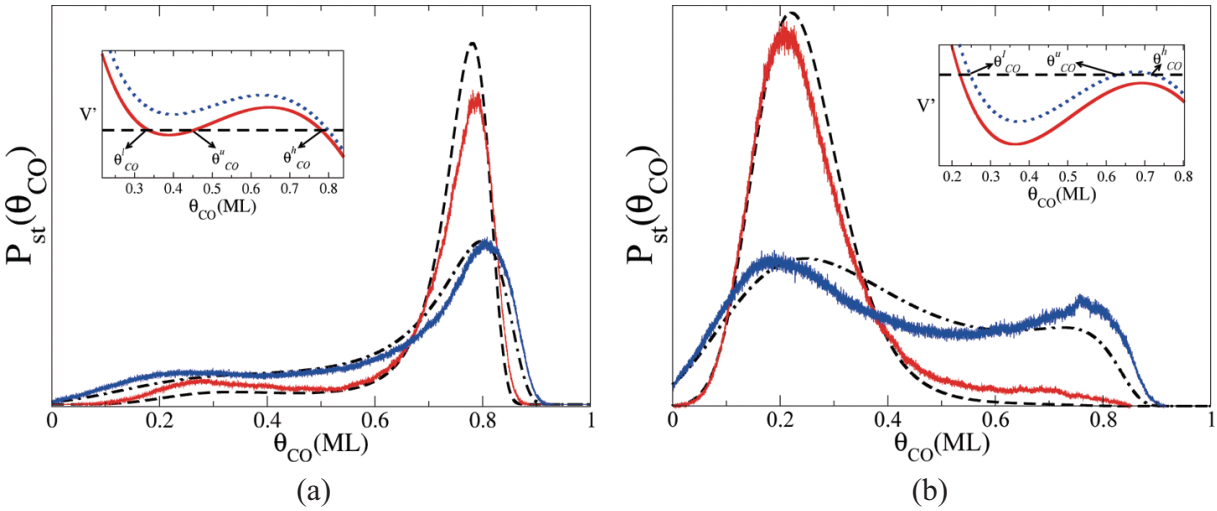

Fig. 3. The main figures show the probability distribution functions of $\theta_{\rm CO}$ from theory for $r = 0.1$ (black dashed lines) and $r = 0.2$ (black dotted dashed lines) and corresponding stochastic simulations of Eqs (1) and (2) (colored solid lines) for parameters around the borders of the bistable region. (a) At $Y = 0.370$ and increasing the noise intensity, a transition from bistability to monostability occurs. (b) When $Y = 0.345$, noise induces a transition from monostability to bistability. Those transitions indicate that the whole bistable region moves toward low values of Y, in agreement with Fig. 2. The insets show $V'(\theta_{\rm CO})$ vs $\theta_{\rm CO}$ for parameters mentioned above. Red solid lines are for $r = 0.1$ and blue dotted lines are for $r = 0.2$. The intersections of $V'(\theta_{\rm CO})$ with the black dashed line are the maxima and minima of the steady state probability distribution functions. The surface temperature is $T = 435K$.

(main figure, black dotted dashed line). This result is confirmed by the probability distributions obtained after numerical integration of the two Langevin equations (Eqs (1) and (2)), for $r = 0.1$ and 0.2. The same behavior occurs in Fig. 3(b) where, starting from a monostable steady state with $Y = 0.345$ (bottom saddle node bifurcation line) and $r = 0.1$ (red solid line), the inset shows that a transition occurs to a bistable state when $r = 0.2$ (blue dotted line), as again confirmed by the numerical integration. In conclusion, the whole bistable region suffers a shift toward low values of Y. This result confirms the bistability bifurcation diagrams presented in Fig. 2.

Figure 4 shows the probability distribution $P_{\rm st}(\theta_{\rm CO})$ (Eq. (10)) and the effective potential $V(\theta_{\rm CO})$ in the bistable and the monostable active and inactive regions for $r = 0.1$. Black dashed lines correspond to the theory and red solid lines to simulation of the whole system. Figure 4(a) shows $P_{\rm st}(\theta_{\rm CO})$ in the monostable reactive and inactive regions as well as inside the bistable region where these two regimes coexist. The corresponding effective potential is also presented in Fig. 4(b). The agreement between theory and simulations coming from the whole system of Langevin equations is good.

Now, it is instructive to show how $P_{\rm st}(\theta_{\rm CO})$ and $V(\theta_{\rm CO})$ change their shapes when approaching the cusp bifurcation point along the equistability line defined as the line where the two local minima have the same level of potential, $V(\theta^h_{\rm CO}) = V(\theta^l_{\rm CO})$. We use for this case a noise intensity of $r = 0.1$ (see Fig. 5). Figure 5(a) shows that well apart from the cusp point, both extrema are well separated by a minimun. But, close to this critical point, where the unstable solution and the two stable ones merge, the fluctuations and the transitions between states increase. Black dashed lines are theoretical results and red solid lines simulations of the whole set of stochastic equations. Note that in both cases the effective potential also gives us an idea of how the external noise affects the transitions between states (see Fig. 5(b)).

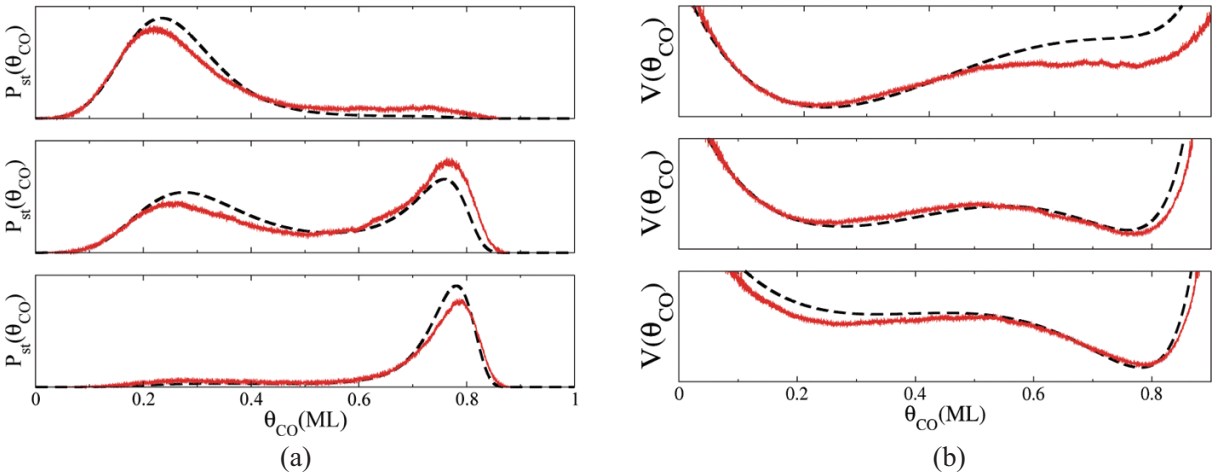

Fig. 4. Comparison of $P_{\rm st}(\theta_{\rm CO})$ and $V(\theta_{\rm CO})$ with same quantities obtained from direct stochastic simulation of the two coupled Langevin equations. The black dashed lines are theoretical results. The red solid lines are stochastic simulations. (a) The probability distribution functions. (b) The effective potentials. In both figures, $Y = 0.3500$, 0.3615, and 0.3700 from top to bottom. The surface temperature and noise intensity are $T = 435K$ and $r = 0.1$, respectively.

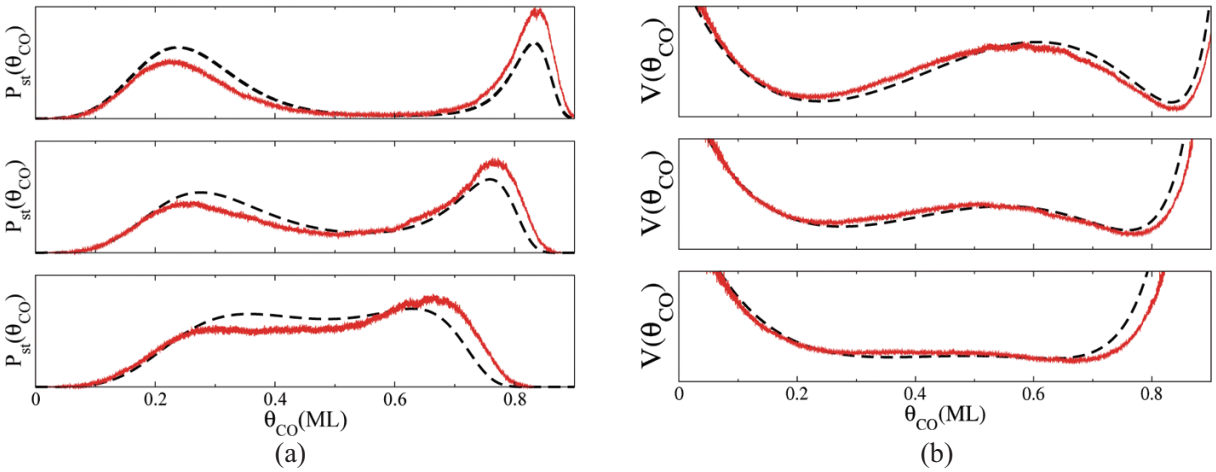

Fig. 5. Distance to the cusp point and the effects on the transitions between stable states. (a) The probability distribution functions. (b) The effective potentials. Along the equistability line, the control parameters are $(Y, T) = (0.3275,430)$, (0.3615,435), and (0.3944,440) from top to bottom. The noise intensity is fixed at $r = 0.1$. Black dashed lines are theoretical results and red solid lines represent stochastic simulations of the two Langevin equations.

Figure 6 presents the potential barrier, $\Delta V = V(\theta^u_{\rm CO}) - V(\theta^l_{\rm CO})$, near the cusp point for values of T and Y alone the equistabiliy line. This figure shows that the barrier vanishes quadratically as T approaches the critical point T_c (see Fig. 6(a)), a result that is qualitatively confirmed in Fig. 6(b) by comparing theoretical values of $V(\theta_{\rm CO})$ (black dashed lines) with numerical values obtained from simulations of the original set of Langevin equations (colored solid lines).

The results presented until now show that, increasing the external noise intensity or approaching the cusp point, the transitions between the stable steady states become more frequent and all possible coverages are populated with nonvanishing probability. The probability distribution and the effective potential

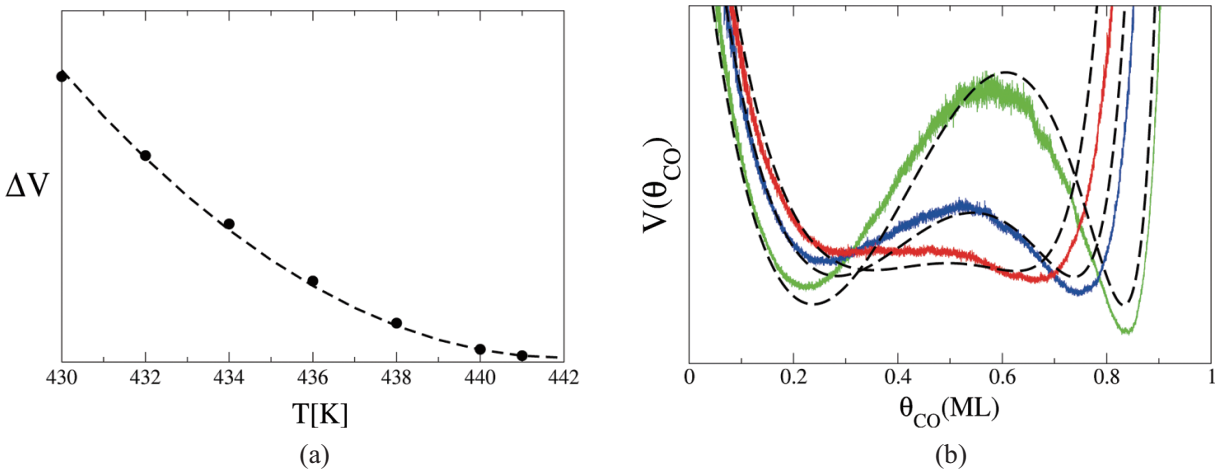

Fig. 6. (a) The barrier high of the effective potential from theory along the equistability line. The control parameters are $(Y, T) = (0.3274,430)$, $(0.3408,432)$, $(0.35423,434)$, $(0.3677,436)$, $(0.3810,438)$, $(0.3941,440)$ and $(0.4005,441)$. Dotted black line is a fit to $\tilde{a}(T_c - T)^2$, where $T_c = 442K$. (b) The effective potential from simulations (colored solid lines) and theory (black dashed lines). The control parameters are $(Y, T) = (0.3274,430)$, $(0.3677,436)$, and $(0.3941,440)$ from top to bottom. The noise intensity is fixed at $r = 0.1$.

associated to our surface reaction model under Gaussian white noise allow us to express the transition times between the reactive ($\theta^l_{\rm CO}$) and inactive ($\theta^h_{\rm CO}$) stable states as [20,21]:

$$t^{lh}(\theta_{\rm CO}) = \int_{\theta^l_{\rm CO}}^{\theta^h_{\rm CO}} d\theta^{'}_{\rm CO} \frac{2}{r^2 \left[g^{\rm CO}(\theta^{'}_{\rm CO})\right]^2 P_{\rm st}(\theta^{'}_{\rm CO})} \int_0^{\theta^{'}_{\rm CO}} d\theta^{''}_{\rm CO} P_{\rm st}(\theta^{''}_{\rm CO}). \tag{13}$$

Figure 7 shows transition times from theory and simulations of the whole system when approaching the cusp point along the equistability line for $r = 0.1$. As expected, the two stable states merge when $T \to T_c$ and the transitions induced by noise become more frequent. Figure 7(a) shows theoretical results after solving Eq. (13). Figures 7(b), (c), and (d) show time series coming from simulations of the two dimensional stochastic system. The red dotted lines represent the solutions of Eq. (12) or the location of the maxima of the corresponding probability distribution function.

5. Summary and conclusions

In this article, we have studied the impact of an external homogeneous Gaussian white noise imposed on a mean-field model for the bistable catalytic CO oxidation on Pd(111) surfaces. Similar to recent experimental studies [6,7,9,11,12], the mean-field model was constructed in a fashion where the total CO+O_2 flux ($\phi = \phi_{\rm CO} + \phi_{\rm O}$) was held constant and CO ($Y = \phi_{\rm CO}/\phi$) and O_2 ($1 - Y$) partial contributions varied. To understand the impact of external noise on the kinetic, we introduced a set of coupled Langevin equations where the external noise is superimposed on the fraction of CO (Y) in the constant gas flow directed at the surface. It was shown that an adiabatic elimination of the fast oxygen coverage is possible. This elimination allows us to get the one component Langevin equation for CO. From the reduced equation, we derived the stationary probability distribution function and introduced an effective potential that can be used to quantify the impact of external noise on the kinetic bistability of CO oxidation on Pd(111) surfaces. We showed analytically and by numerical simulations that a shift of the bistable region occurs when the external noise intensity varies.

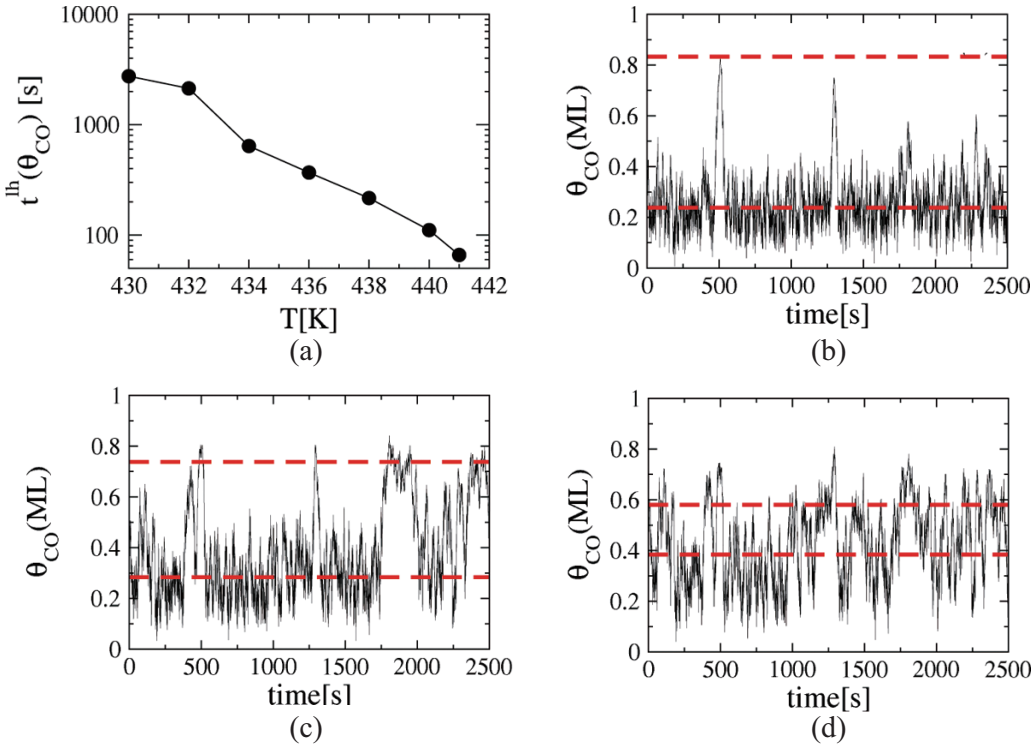

Fig. 7. Qualitative comparison of the transition times between the active and inactive state obtained from theory and stochastic simulations of the two Langevin equations. (a) Theoretical transition times $t^{lh}(\theta_{\rm CO})$ approaching the cusp point along the equistability line. (b) Time series showing transitions between steady states for $(Y,T) = (0.3274,430)$. (c) Time series showing transitions for $(Y,T) = (0.3677,436)$. (d) Time series and transitions for $(Y,T) = (0.4005,441)$. The noise intensity is $r = 0.1$. Red dashed lines represent stable solutions as obtained from Eq. (12).

We found that the transitions between the active and inactive states of the bistable region become more frequent approaching the cusp point. It was found that the barrier height of the effective potential behaves as $\Delta V \sim (T_c - T)^2$, in agreement with the Landau prediction for mean-field models [22]. The transition times between the stable states are also calculated theoretically from the steady state probability distribution. The theoretical predictions derived from the reduced model have been found to be in reasonable agreement with a numerical simulation of the original coupled Langevin equations.

Although, the stochastic description presented in this paper describes very well the impact of a homogeneous external Gaussian white noise on the kinetic bistability of CO oxidation on Pd(111), future new studies should include correct adparticle diffusion in order to understand the impact of external noise on the great variety of spatiotemporal patterns observed in these surface reactions. In this situation one has to distinguish between spatially homogeneous noise and spatiotemporal noise. It is also known that the surface of the crystal is not really homogeneous because there are heterogeneities (point defects, atomic steps, kink sites or extended microfacets) that affect the diffusion of adparticles. Such heterogeneities introduce a new source of internal noise that should be taken into account in more realistic models [12]. The transition times will be also affected by these heterogeneities. In real situations, to go from one state to the other, the system can first nucleate a domain of the other state. Then the domain can grow and spread over the whole system. To extend the adiabatic reduction technique used in this paper to the case of stochastic reaction-diffusion systems is also an interesting challenge in surface reactions. The case of external colored noise and non-Gaussian white noise may be also considered in future works [1,23].

An interesting extension is to use stochastic analysis to study the impact of external noise on the catalytic CO oxidation on nanoscale surfaces, where molecular noise plays an important role [4,5]. The results presented in this paper could also stimulate new theoretical and experimental studies in order to understand the role of noise in other nonlinear catalytic reactions on single crystal surfaces [2,24,25]. We also believe that new experiments could show the phenomena predicted in this paper for the kinetic bistability of CO oxidation on Pd(111).

Finally, it is instructive to mention that Erban et al. [26] have used similar adiabatic reduction methods in gene regulatory networks to get effective potentials for assessing bistability. They used recursive projection methods and data-mining based techniques that find approximate low-dimensional inertial manifolds.

Acknowledgments

M.P. gratefully acknowledge support from USB-DID. This work was supported by MINECO (Spain), Comunitat Autònoma de les Illes Balears, FEDER, and the European Commission under projects FIS2007-60327 and FIS2012-30634.

References

[1] F. Sagués, J.M. Sancho and J. Garcia-Ojalvo, Spatiotemporal order out of noise, *Rev Mod Phys* **79** (2007), 829.
[2] R. Imbihl and G. Ertl, Oscillatory kinetics in heterogeneous catalysis, *Chem Rev* (Washington, D.C) **95** (1995), 697.
[3] R. Imbihl, Nolinear dynamics on catalytic surfaces: The contribution of surface science, *Surface Science* **603** (2009), 1671.
[4] V. Johanek, M. Laurin, A.W. Grant, B. Kasemo, C.R. Henry and J. Libuda, Fluctuations and bistabilities on catalyst nanoparticles, *Science* **304** (2004), 1639.
[5] Y. Suchorski, J. Beben, E.W. James, J.W. Evans and R. Imbihl, Fluctuations-induced transitions in a bistable surface reaction: Catalytic CO oxidation on a Pt field emitter tip, *Phys Rev Lett* **82** (1999), 1907.
[6] S. Wehner, P. Hoffmann, S. Schmeisser, H.R. Brand and J. Küppers, Spatiotemporal patterns of external noise-induced transitions in a bistable reaction-diffusion systems: Photoelectron emission microscopy experiments and modeling, *Phys Rev Lett* **95** (2005), 038301.
[7] S. Wehner, Y. Hayase, H.R. Brand and J. Küppers, Multiplicative temperature noise applied to a bistable surface reaction: Experiment and theory, *J Phys Chem B* **108** (2004), 14452.
[8] P.S. Bodega, S. Alonso and H.H. Rotermund, Effects of external global noise on the catalytic CO oxidation on Pt(110), *J Chem Phys* **130** (2009), 084704.
[9] Y. Hayase, S. Wehner, J. Küppers and H.R. Brand, External noise imposed on the reaction-diffusion system $CO+O_2\rightarrow CO_2$ on Ir(111) surfaces: Experiment and theory, *Phys Rev E* **69** (2004), 021609.
[10] T. Engel and G. Ertl, A molecular beam investigation of the catalytic oxidation of CO on Pd(111), *J Chem Phys* **69** (1978), 1267.
[11] S. Karpitschka, S. Wehner and J. Küppers, Reaction hysteresis of the $CO+O_2\rightarrow CO_2$ reaction on palladium(111), *J Chem Phys* **130** (2009), 054706.
[12] S. Wehner, S. Karpitschka, Y. Burkov, D. Schmeiser, J. Küppers and H.R. Brand, Stochastic aspects of pattern formation during the catalytic oxidation of CO on Pd(111) surfaces, *Physica D* **239** (2010), 746.
[13] C.W. Gardiner, *Handbook of Stochastic Methods for Physics, Chemistry and the Natural Science*, Springer-Verlag, Berlin, 1985.
[14] P. Kloeden and E. Platen, *Numerical Solutions of Stochastic Differential Equations*, Springer, Berlin, 1999.
[15] T. Turanyi, A. Tomlin and M. Pilling, On the error of the quasi-steady approximation, *J Phys Chem* **97** (1993), 163.
[16] E. Knobloch and K. Wiesenfeld, Bifurcations in fluctuating systems: The center-manifold approach, *J Stat Phys* **33** (1983), 611.
[17] Y. Lan, T.C. Elston and G.A. Papoian, Elimination of fast variables in chemical Langevin equations, *J Chem Phys* **129** (2008), 214115.
[18] M. Pineda and R. Toral, External noise induced phenomena in CO oxidation on single crystal surfaces, *J Chem Phys* **130** (2009), 124704.

[19] W. Horsthemke and R. Lefever, *Noise Induced Transitions, Springer*, Berlin, 1984.
[20] A.J.R. Madureira, P. Hänggi, V. Buonomano and W.A. Rodrigues, Jr., Escape from a fluctuating double well, *Phys Rev E* **51** (1995), 3849.
[21] P. Hänggi, Escape from a metastable state, *J Stat Phys* **42** (1986), 105.
[22] D.J. Liu and J.W. Evans, Fluctuations and bistability in a "hybrid" atomistic model for CO oxidation on nanofacets: An effective potential analysis, *J Chem Phys* **117** (2002), 7319.
[23] J. Cisternas, R. Lecaros and S. Wehner, Carbon monoxide oxidation on Iridium(111) surfaces driven by strongly colored noise, *Eur Phys J D* **62** (2011), 91.
[24] H. Rose, H. Hempel and L. Schimansky-Geier, Stochastic dynamics of catalytic CO oxidation on Pt(100), *Physica A* **206** (2004), 421.
[25] J.-S. McEwen, P. Gaspard, T. Visart de Bocarmé and N. Kruse, Nanometric chemical clocks, *Proc Natl Acad Sci USA* **106** (2009) 3006.
[26] R. Erban, T. Frewen, X. Wang, T. Elston, R. Coifman, B. Nadler and I. Kevrekidis, Variable-free exploration of stochastic models: A gene regulatory network example, *J Chem Phys* **126** (2007), 155103.